

The Enthalpies of Formation for Polychlorinated Dibenzofurans with Use of G3XMP2 Model Chemistry and Density Functional Theory

Liming Wang* and Yi-Liang He

College of Chemistry and Chemical Engineering, South China University of Technology, Guangzhou 510640, China

Received: March 10, 2008; Revised Manuscript Received: October 18, 2008

The standard gas-phase enthalpies of formation of polychlorinated dibenzofurans (PCDFs) have been predicted by using G3XMP2 model chemistry, density functional theory (DFT), and second-order Muller-Plesset (MP2) theory, coupled with isodesmic reactions. The results show a large difference between G3XMP2 and DFT methods with 6-31G(2df,p) and 6-311++G(3df,3pd) basis sets, while MP2/G3MP2 Large calculations agree closely with G3XMP2. Two isodesmic reaction schemes are used for better prediction of formation enthalpies. The first (IR1) employs monochlorobenzene as a reference species and the second (IR2) employs polychlorinated benzenes as reference species. The relative stability of PCDFs is rationalized by positional interactions. While the Cl-substitution at position 1/9 leads to the most stable isomers, the simultaneous substitutions at positions 1 and 9 result in a strong repulsion between Cl atoms. Failure of DFT-B3LYP is due to the overestimation of *o*-ClCl repulsion. For 1,9-PCDFs, the torsion motions of the benzene rings have extremely low harmonic vibrational frequencies. Their contributions to entropy, heat capacity, and thermal corrections have been calculated by using the numerically evaluated energy levels. The PCDF isomer patterns are also discussed based on the calculated thermodynamic parameters.

I. Introduction

The formation of polychlorinated dibenzo-*p*-dioxins (PCDDs) and dibenzofurans (PCDFs) from municipal waste incinerators (MWIs) has received extensive study due to their strong toxicity. The formation mechanisms usually proposed include the gas-phase condensation of chlorinated phenols and benzenes, and fly ash-mediated and/or metal-catalyzed reactions of chlorinated phenols, benzenes, acetylene, polycyclic aromatic hydrocarbons (PAHs), soot, etc.^{1–4} In addition, chlorination of less chlorinated congeners produced in the gas phase and dechlorination of highly chlorinated congeners produced by de novo synthesis are also introduced to account for the isomer pattern.^{5–7} Researches have focused on the formation mechanisms and the possible strategies in reducing the productions of chlorinated aromatics.

PCDD/Fs emitted from MWIs appear to have a quite consistent chlorination pattern within homologues across various samples and conditions. This is an argument in favor of thermodynamic control of the isomer distribution in de novo formation processes.^{2,8} Thermodynamic properties are also important parameters in understanding their gas phase phenol condensation mechanism.^{9–11} Without reliable information, modeling of these processes has been based on roughly estimated kinetic and thermodynamic parameters.^{9,12}

The experimental measurements on thermodynamic properties of PCDD/Fs are rather limited and none for the enthalpy of formation of PCDFs up to now,^{13,14} except for dibenzofuran (DBF) itself.^{15–17} Alternatively, the properties have been predicted by using the empirical group additivity method,^{18–22} semiempirical molecular orbital methods,^{23–25} density functional theory (DFT) methods,^{26–30} and recently Gaussian-3X (G3X) model chemistry,³¹ where DFT and G3X calculations are usually coupled with isodesmic reactions to minimize the deficiency in treating electron correlation. Rather large discrepancies have been found among different methods, e.g.,

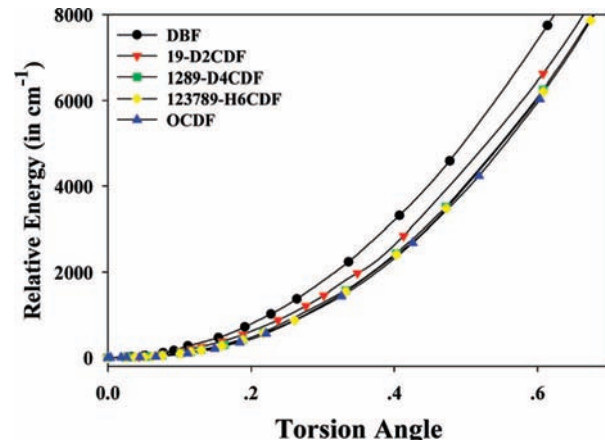


Figure 1. The ring-torsion potential energy profiles of DBF, 1,9-D₂CDF, 1,2,8,9-T₄CDF, 1,2,3,7,8,9-H₆CDF, and OCDF at the B3LYP/6-31G(2df,p) level.

ΔH_{298K}° (O₈CDF) has been predicted as -182.8,¹⁸ -63.7,¹⁹ -125.8,²⁰ -130,²¹ and -161 ± 35 kJ/mol²⁷ from group additivity approaches, -50.5 kJ/mol from MNDO²³ and -55.1 kJ/mol from PM3²⁵ calculation, and -15,²⁹ -23,²² and -60³⁰ kJ/mol from DFT calculations. Our recent study on the enthalpies of formation of chlorinated benzenes, phenols, and PCDDs shows that DFT-B3LYP predictions are much higher than G3X and G3XMP2 predictions.³¹ The purpose of the present study is to predict the enthalpies of formation of PCDFs by using G3XMP2 model chemistry and DFT methods.

II. Computational Methods

G3XMP2 model chemistry³² is used for the prediction of the enthalpies of formation of PCDFs. The geometries are optimized at the DFT-B3LYP/6-31G(2df,p) level, and the vibrational frequencies are evaluated at the same level of theory and scaled

* Corresponding author. Phone: +86 20 87112900. Fax: +86 20 87112906. E-mail: wanglm@scut.edu.cn.

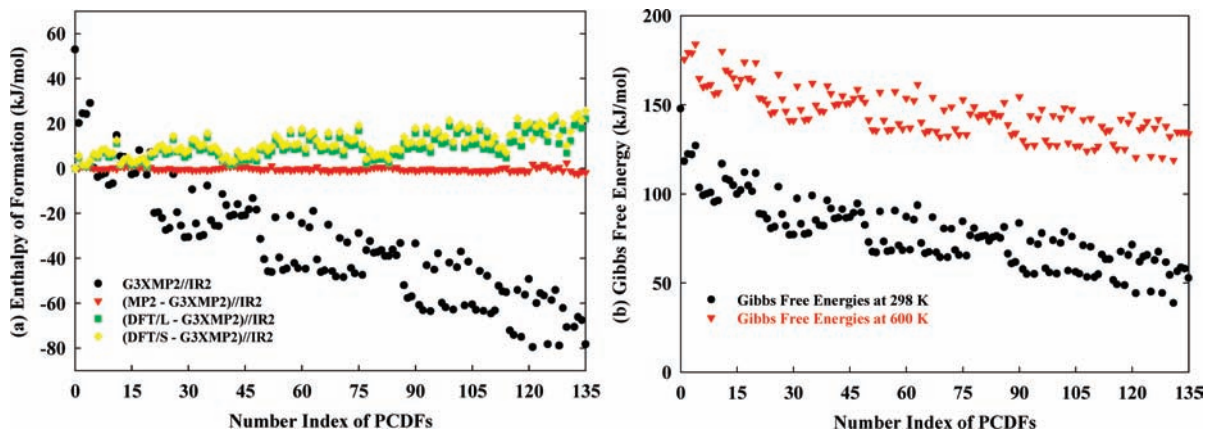


Figure 2. (a) The enthalpies of formation of PCDFs at the G3XMP2//IR2 level, and the differences of B3LYP, MP2, and PM3 to G3XMP2, where B3LYP/L = B3LYP/6-311++G(3df,3pd), B3LYP/S = B3LYP/6-31G(2df,p), and MP2 = MP2/G3MP2Large; (b) the standard Gibbs free energies at 298 and 600 K.

TABLE 1: Molar Entropy (S , in $\text{J K}^{-1} \text{ mol}^{-1}$) and Thermal Correction ($H^T - H^0$, in kJ mol^{-1}) of the Benzene-Ring Torsion Modes

		298.15	300	400	500	600	800	1000	1200	1500	2000
DBF	S^a	15.63	15.68	18.05	19.88	21.39	23.76	25.60	27.09	28.88	31.00
	$H^T - H^0a$	2.00	2.01	2.83	3.66	4.48	6.13	7.78	9.42	11.81	15.49
	S^b	13.80	13.85	16.21	18.04	19.55	21.93	23.78	25.29	27.15	29.54
	$H^T - H^0b$	1.89	1.91	2.72	2.72	4.35	6.03	7.69	9.35	11.84	15.99
1,9-D ₂ CDF	S^a	21.97	22.02	24.36	26.16	27.62	29.82	31.38	32.49	33.62	34.69
	$H^T - H^0a$	2.23	2.24	3.05	3.86	4.66	6.19	7.58	8.80	10.31	12.16
	S^b	24.08	24.13	26.52	28.37	29.89	32.28	34.13	35.65	37.50	39.90
	$H^T - H^0b$	2.30	2.31	3.14	3.97	4.80	6.47	8.13	9.79	12.29	16.44
1,2,8,9-T ₄ CDF	S^a	23.20	23.25	25.50	27.24	28.65	30.87	32.58	33.96	35.59	37.50
	$H^T - H^0a$	2.21	2.22	3.01	3.78	4.56	6.10	7.64	9.15	11.33	14.63
	S^b	29.84	29.89	32.28	34.14	35.65	38.05	39.90	41.42	43.27	45.66
	$H^T - H^0b$	2.39	2.40	3.23	4.07	4.90	6.56	8.22	9.88	12.38	16.54
1,2,3,7,8,9-H ₆ CDF	S^a	24.73	24.78	27.03	28.76	30.17	32.38	34.07	35.40	36.93	38.61
	$H^T - H^0a$	2.24	2.25	3.03	3.81	4.58	6.11	7.63	9.09	11.14	14.05
	S^b	33.42	33.48	35.87	37.72	39.24	41.63	43.48	45.00	46.86	49.25
	$H^T - H^0b$	2.42	2.43	3.27	4.10	4.93	6.59	8.25	9.92	12.41	16.57
O ₈ CDF	S^a	32.88	32.98	35.04	36.58	37.72	39.22	40.11	40.67	41.17	41.59
	$H^T - H^0a$	2.24	2.26	2.99	3.67	4.30	5.34	6.13	6.74	7.41	8.139
	S^b	39.40	39.45	41.84	43.70	45.22	47.61	49.46	50.98	52.83	55.23
	$H^T - H^0b$	2.45	2.47	3.30	4.13	4.96	6.62	8.29	9.95	12.44	16.60

^a From summation over the numerically evaluated energy levels, with the following parameters for potential energy profiles: DBF ($k_2 = 19613$, $k_4 = 1521$, $k_6 = 5038$, $k_8 = -8146$, and $k_{10} = 4305$, all in cm^{-1}); 1,9-D₂CDF ($k_2 = 14684$, $k_4 = 16681$, $k_6 = -35575$, $k_8 = 46949$, $k_{10} = -23648$, all in cm^{-1}), 1,2,8,9-T₄CDF ($k_2 = 10553$, $k_4 = 43790$, $k_6 = -125438$, $k_8 = 179808$, $k_{10} = -94434$, all in cm^{-1}); 1,2,3,7,8,9-H₆CDF ($k_2 = 10207$, $k_4 = 44008$, $k_6 = -121574$, $k_8 = 169320$, $k_{10} = -87153$, all in cm^{-1}); and OCDF ($k_2 = 7518$, $k_4 = 103776$, $k_6 = -602399$, $k_8 = 1715727$, $k_{10} = -1803279$, all in cm^{-1}). ^b Using harmonic-oscillator approximation.

by 0.9854 for zero-point energy (ZPE) corrections and thermal corrections. The G3XMP2 electronic energies are approximately at the electron correlation level of QCISD(T)/G3ExtraLarge. These calculations are carried out by using the Gaussian 03 suite of program.³³ Electronic energies are also evaluated at the B3LYP level with a large basis set of 6-311++G(3df,3pd), using the NWChem 5.0 package³⁴ with a medium grid to achieve energy accuracy of 1×10^{-6} hartree. The B3LYP/6-31G(2df,p) vibrational frequencies and rotational constants, ZPEs, and electronic energies are listed in the Supporting Information.

III. Results and Discussions

A. The Low-Frequency Vibrational Modes. PCDFs possess a few low-frequency vibrational modes. The most prominent ones are the torsion motion and the butterfly motion of the two benzene rings. The calculated harmonic frequencies for the torsion modes are extremely low, especially when sites 1 and 9 are both chlorinated, e.g., 5 cm^{-1} in O₈CDF, 8 cm^{-1} in 1,2,3,4,7,8,9-H₆CDF, and 10 cm^{-1} in 1,2,3,7,8,9-H₆CDF; while the frequencies of the butterfly modes are relatively higher, e.g., 38 cm^{-1} for O₈CDF, 39 cm^{-1} for 1,2,3,4,7,8,9-H₆CDF, and 40 cm^{-1} for 1,2,3,7,8,9-H₆CDF (see the Supporting Information). While the butterfly modes can be treated approximately as harmonic oscillators (HOs), the torsion motions with extremely low frequencies require further consider-

ation. The potentials of the torsion motions should be described as a mixing of quadratic and high-order terms as

$$V(\delta) = k_2 \delta^2 + k_4 \delta^4 + k_6 \delta^6 + k_8 \delta^8 + \dots$$

where δ is the torsion angle. The corresponding kinetic energy for these modes is

$$E(\delta) = \frac{1}{2} I \dot{\delta}^2$$

where I is approximated as the rotational momentum of inertia relative to the long principal axis in the molecular plane, excluding the contribution from the O-atom. We have obtained the potential profiles for DBF and several 1,9-PCDFs at the B3LYP/6-31G(2df,p) level with other coordinates relaxed (Figure 1). The potential profiles are relatively flat at small torsion angles and increase sharply at large torsion angles. The Schrödinger equation of these modes is solved numerically by using the Fourier Grid Hamiltonian (FGH) method,³⁵ and the energy levels are used to calculate the partition function, the entropies, and the thermal corrections, which are significantly different from those predicted by using the harmonic-oscillator approximation (Table 1). The contribution of high-order terms to the potential energies increases from 1,9-D₂CDF to O₈CDF; thereafter, the differences in entropies and thermal corrections between FGH and HO increase gradually as

TABLE 2: Molar Entropy and Heat Capacity of Dibenzofuran (all in $J\ K^{-1}\ mol^{-1}$)

T	C_p^a	C_p^b	C_p^c	T	S^a	S^b	T	S^a	S^d	S^e	S^f
200	104.49	104.58	103.1	200	323.24	324.00	298.15	375.79	377.62	374.4	375.9
250	133.99	133.95	250	349.69	350.52	300	376.80	376.80	378.63	375.8	376.9
298.15	163.16	163.05	160.5	298.15	375.79	376.54	320	387.79	389.62	387.0	387.9
300	164.27	164.21	161.7	300	376.80	377.62	340	398.82	400.65	398.3	398.9
400	220.79	220.83	217.5	400	432.00	432.74	360	409.88	411.71	409.7	410.0
500	267.58	267.83	264.1	500	486.68	487.28	380	420.94	422.78	421.0	421.1
600	304.67	305.12	301.2	600	538.68	539.58	400	432.00	433.84	432.2	432.1
800	357.70		354.6				420	443.02	444.86	443.4	443.1
1000	393.10		390.5				440	453.99	455.83	454.5	454.1
1200	417.97						460	464.90	466.74	465.5	465.0
1500	443.15		441.3				480	475.73	477.58	476.5	475.9
2000	467.25		466.0				500	486.48	488.33	487.4	486.6
2500			479.4				520	497.14	498.98	498.2	497.2
							540	507.69	509.53	508.9	507.8
							560	518.14	519.98	519.5	518.2
							580	528.47	530.41	530.0	528.6
							600	538.68	540.52	540.4	538.8
							620	548.78	550.62	550.8	548.9
							640	558.75	560.59	561.1	558.9
							660	568.60	570.44	571.3	568.7
							680	578.33	580.17	581.5	578.5
							700	587.94	589.78	590.3	588.1
							720	597.42	599.26	601.6	597.6

^a Present work with RRHO approximation, using B3LYP/6-31G(2df,p) geometry and vibrational frequencies (scale factor 0.9854).

^b Calculation with RRHO approximation, using experimental vibrational frequencies and X-ray structures, by Klots et al. (ref 14). ^c Calculation with RRHO approximation, using B3LYP/6-31G(d,p) geometry and vibrational frequencies, by Zhu et al. (ref 26). ^d Present work, calculation with the torsion mode treated numerically (see Section III.A). ^e “Calorimetric” determination, by Chirico et al. (ref 17). ^f Calculations with RRHO approximation, using experimental vibrational frequencies, by Dorofeeva et al. (ref 27).

TABLE 3: The Enthalpy of Formation of Dibenzofuran from Reaction Scheme at 298 K at the G3X, G3XMP2, and B3LYP Levels (all in kJ/mol)^a

reactions ^b	G3X	G3XMP2	B3LYP ^c	lit. value
1. DBF + 16CH ₄ + H ₂ O → 7C ₂ H ₆ + 6C ₂ H ₄ + 2C ₂ H ₅ OH ^d	53.1	64.2	62.6	69.0 ^d
2. DBF + C ₂ H ₄ → C ₈ H ₈ O + C ₆ H ₆	46.9	48.8	58.1	58.2 ^e
3. DBF + 3H ₂ → 2C ₆ H ₆ + H ₂ O	35.8	31.6	65.2	63.6 ^f
4. DBF + 2H ₂ → C ₆ H ₆ OH + C ₆ H ₆	37.4	33.9	65.1	64.0 ^f
5. DBF + H ₂ O + H ₂ → 2C ₆ H ₅ OH	37.6	34.3	57.5	64.4 ^f
6. DBF + 2C ₂ H ₄ → 2C ₆ H ₆ + C ₄ H ₆ O	41.0	44.4	62.2	61.5 ^f
7. DBF + C ₂ H ₆ → C ₈ H ₈ O + C ₆ H ₆	52.8	55.3	64.6	58.2 ^f
8. DBF + 2C ₂ H ₄ + H ₂ → 2C ₆ H ₆ + CH ₂ =CHOCH=CH ₂	40.5	40.3	70.9	
average	43.1 ± 6.9	44.1 ± 11.5	63.3 ± 4.3	

^a G3X, G3XMP2, and B3LYP are based on geometries and ZPEs at B3LYP/6-31G(2df,p). ^b Experimental values (in kJ/mol) are from the NIST Web site unless otherwise stated: H₂O (-241.8), CH₄ (-74.87), C₂H₄ (52.47), C₂H₆ (-83.8), CH₃OH (-201.0), C₆H₆ (82.6), C₆H₅OH (-96.4), C₈H₈O (benzofuran, 13.6 ± 0.7), C₈H₈O (2,3-dihydrobenzofuran, -46.5 ± 0.8), C₂H₃OC₂H₃ (-12.7 ± 0.84).

^c B3LYP = B3LYP/6-311+G(3df,2p). ^d G3MP2 level (ref 40).

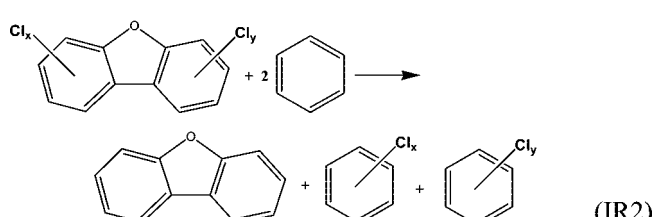
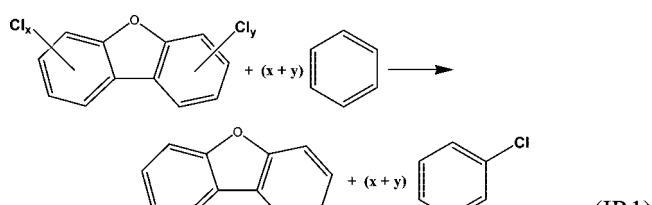
^e B3LYP/6-311+G(3df,2p) with B3LYP/6-31G(d) geometries and ZPEs (refs 26 and 42). ^f B3LYP/6-311+G(3df,2p) with B3LYP/6-31G(d) geometries and ZPEs (refs 26 and 42).

well. Nevertheless, the thermal corrections at 298 K from FGH and HO are within 0.3 kJ/mol.

The entropies and heat capacities of PCDFs are first evaluated here by using rigid-rotor-harmonic-oscillator (RRHO) approximation (see the Supporting Information). For DBF, the B3LYP harmonic frequency of the torsion mode is 110 cm⁻¹; thereafter, the predicted entropies and heat capacities using FGH and HO results agree closely with the previous calorimetric measurements,¹⁷ calculations with experimental vibrational frequencies,^{14,27} and group additivity estimations.^{19,36} For PCDFs not being chlorinated

at sites 1 and 9 simultaneously, our calculations with RRHO approximation agree closely with those by Dorofeeva et al.,²⁷ e.g., $C_{p,298K}$ of 226.3 and 242.3 J K⁻¹ mol⁻¹ by us vs 225.9 and 241.1 J K⁻¹ mol⁻¹ by Dorofeeva et al. and S_{298K} of 498.9 and 528.8 J K⁻¹ mol⁻¹ by us vs 496.5 and 525.7 J K⁻¹ mol⁻¹ by Dorofeeva et al. for 1,2,6,7-T₄CDF and 1,2,4,7,8-P₅CDF, respectively. For O₈CDF, $C_{p,298K}$ of 287.9 J K⁻¹ mol⁻¹ from our RR-FGH calculations agrees with that of 289.7 J K⁻¹ mol⁻¹ from RRHO calculations by Dorofeeva et al., while S_{298K} of 617.3 J K⁻¹ mol⁻¹ from RR-FGH is higher than that of 603.7 J K⁻¹ mol⁻¹ from RRHO by Dorofeeva et al. Overall, it is necessary to treat the extremely low-frequency torsion modes with high-order potentials for reliable predictions of entropies, heat capacities, and the thermal corrections at high temperatures, whereas RRHO is good enough for enthalpies of formation at 298 K.

B. Enthalpy of Formation of Dibenzofuran. The experimental thermodynamic properties of PCDFs are available to none-substituted dibenzofuran only. The enthalpies of formation for PCDFs can be obtained directly from the G3XMP2 atomization energies; however, large errors are expected as for the cases of chlorinated phenols and PCDDs.³¹ It is therefore necessary to employ proper isodesmic reactions. Two reactions have often been used:^{11,19,26–28}



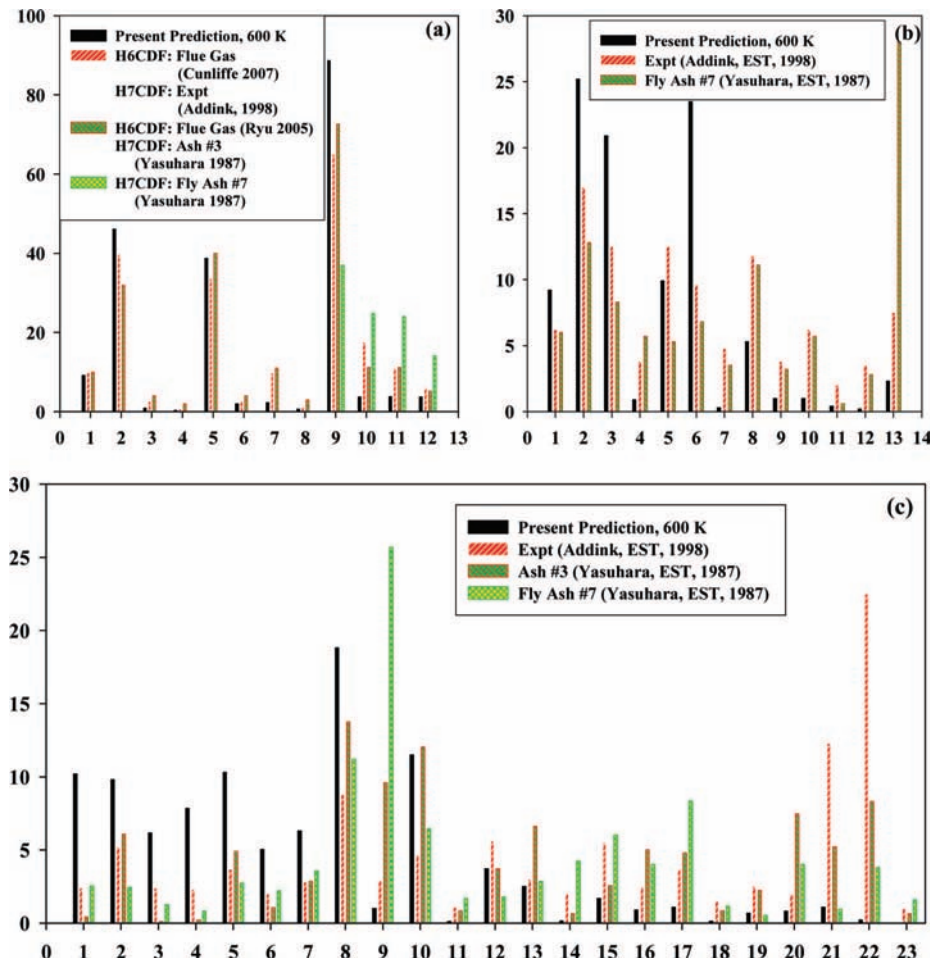


Figure 3. Experimental (Addink et al.,⁸ Cunliffe et al.,⁴⁵ Ryu et al.,⁷ and Yasuhara et al.⁴⁴) and theoretical relative congener abundances: (a) H₆CDFs and H₇CDFs: 1 = 123468, 2 = 124678 + 134678 + 134679, 3 = 124679, 4 = 124689, 5 = 123467 + 123478 + 123678 + 123479, 6 = 123469 + 123679 + 123689, 7 = 234678, 8 = 123489 + 123789-H₅CDF, 9 = 1234678, 10 = 1234679, 11 = 1234689, and 12 = 1234789-H₇CDF; (b) H₆CDFs: 1 = 123468, 2 = 134678 + 134679, 3 = 124678, 4 = 124678, 5 = 123478 + 123479, 6 = 123678, 7 = 124689, 8 = 123467, 9 = 123679, 10 = 123469 + 123689, 11 = 123789, 12 = 123489, 13 = 234678-H₅CDF; (c) H₄CDFs: 1 = 1368, 2 = 1378 + 1379, 3 = 1347, 4 = 1468, 5 = 1247 + 1367, 6 = 1348, 7 = 1346 + 1248, 8 = 1246 + 1268 + 1237 + 1369 + 1478, 9 = 2349 + 1234, 10 = 1238 + 1467 + 2468 + 1236, 11 = 1349, 12 = 1278, 13 = 1267 + 1279, 14 = 1469, 15 = 1249 + 2368, 16 = 2467, 17 = 1239 + 2347, 18 = 1269, 19 = 2378, 20 = 2348, 21 = 2346 = 2367, 22 = 3467, 23 = 1289-T₄CDF.

where IR2 is better balanced on the Cl–Cl interactions within the benzene rings, even though the differences between similar isodesmic reactions on PCDDs are within 3 kJ/mol at the G3XMP2 level. For the use of IR2, the experimental enthalpies of formation for C₆H_{6-n}Cl_n ($n = 0-3$) ($\Delta_fH_{298K}^\circ = 82.6 \pm 0.7$, 52.0 ± 1.3 , 30.2 ± 2.1 , 25.7 ± 2.1 , 22.5 ± 1.5 , 8.2 ± 1.8 , and 4.9 ± 1.6 kJ/mol for C₆H₆, C₆H₅Cl, 1,2-C₆H₄Cl, 1,3-C₆H₄Cl₂, 1,4-C₆H₄Cl₂, 1,2,3-C₆H₃Cl₃, and 1,2,4-C₆H₃Cl₃, respectively)³⁷ and the theoretical prediction for 1,2,3,4-C₆H₂Cl₄ ($\Delta_fH_{298K}^\circ = -8.3$ kJ/mol) are adopted.³¹ Besides these, a reliable value for DBF is required.

Cass et al.¹⁵ first measured $\Delta_fH_{298K}^\circ(\text{DBF}, \text{g}) = 83.2 \pm 4.6$ kJ/mol, which was listed in Cox and Pilcher's compilation in 1970³⁸ and recommended by Pedley in 1994.³⁷ Even though a molecular mechanics prediction of 84.0 kJ/mol with use of the MM3 force field supported this measurement,³⁹ it is generally considered to be too high. Two later combustion measurements resulted in much lower values of 47.6 ± 4.6 kJ/mol by Sabbah et al.¹⁶ and 55.2 ± 0.8 kJ/mol by Chirico et al.¹⁷ The discrepancy between the two measurements arises largely from the measured enthalpy of sublimation with the enthalpy of formation for crystalline DBF differing by only 0.3 kJ/mol. Sabbah et al. obtained $\Delta_{\text{sub}}H_{298K}^\circ = 76.5$ kJ/mol from calorimetry study and the result has been criticized;^{17,40,41} while Chirico et al. obtained

$\Delta_{\text{sub}}H_{298K}^\circ = 84.4$ kJ/mol from the measured vapor pressure from 358 to 603 K. The source of the error in the latter determination arises from the long extrapolation to 298.15 K. The recent study by Verevkin⁴¹ obtained a more reliable $\Delta_{\text{sub}}H_{298K}^\circ = 82.04 \pm 0.24$ kJ/mol from the temperature dependence of the vapor pressure from 292.9 to 352.5 K, being about 2 kJ/mol lower than that by Chirico et al. Together with the enthalpy of formation for crystalline DBF by Chirico et al.,¹⁷ Verevkin obtained $\Delta_fH_{298K}^\circ(\text{DBF}, \text{g}) = 52.90 \pm 0.65$ kJ/mol.

Theoretically, Notario et al.⁴⁰ have obtained $\Delta_fH_{298K}^\circ(\text{DBF}, \text{g}) = 51.9 \pm 6.7$ kJ/mol from the average of G3MP2B3 values using atomization, bond separation isodesmic reactions, and bond-additivity + ring correction schemes. At the B3LYP/6-311+G(3df,2p)//B3LYP/6-31G(d,p) level, Zhu et al.²⁶ obtained a slightly higher value of 58.2 kJ/mol using the isodesmic reaction of DBF + C₂H₄ → benzofuran + C₆H₆, and Altaramen et al.⁴² proposed a value of 59.4 ± 6.3 kJ/mol from six reactions. Here we used all these reactions to derive $\Delta_fH_{298K}^\circ(\text{DBF})$ at G3X, G3XMP2, and B3LYP/6-311+G(3df,2p) levels (Table 1). Large discrepancies are found between G3X, G3XMP2, and B3LYP predictions and between different reactions. The differences between G3X and G3XMP2 are significant, even though the averages over reactions differ by only 1 kJ/mol. Predictions from B3LYP agree slightly better across the reactions, while the

TABLE 4: The Calculated Enthalpies of Formation at 298.15 K, and Gibbs Free Energies at 298 and 600 K (all in kJ/mol) from Atomization and Isodesmic Reactions^a

no.	PCDFs	G3XMP2				MP2		DFT/L		DFT/S		
		AR	IR1	IR2	G-298	G-600	IR1	IR2	IR1	IR2	IR1	IR2
0	0-	37.7	52.9	52.9	147.8	203.2	52.9	52.9	52.9	52.9	52.9	52.9
1	1-	1.4	20.2	20.2	118.3	175.6	20.3	20.3	24.9	24.9	25.8	25.8
2	2-	5.6	24.5	24.5	122.4	179.3	25.5	25.5	25.8	25.8	26.2	26.2
3	3-	5.3	24.2	24.2	122.1	179.1	24.9	24.9	25.0	25.0	25.7	25.7
4	4-	10.2	29.1	29.1	127.0	184.1	29.7	29.7	31.8	31.8	32.6	32.6
5	1,2-	-22.6	0.0	0.2	103.5	164.7	-0.6	0.2	9.9	5.9	12.4	6.8
6	1,3-	-27.6	-5.1	-3.8	99.2	160.0	-5.3	-4.1	0.1	1.0	2.2	2.1
7	1,4-	-23.1	-0.6	-2.9	100.0	160.6	-0.8	-3.2	6.3	4.3	8.4	5.4
8	1,6-	-24.7	-2.2	-2.2	100.7	161.4	-2.3	-2.3	4.7	4.7	6.5	6.5
9	1,7-	-30.1	-7.5	-7.5	95.4	156.1	-7.6	-7.6	-2.6	-2.6	-0.9	-0.9
10	1,8-	-29.3	-6.7	-6.7	96.2	156.9	-6.4	-6.4	-1.1	-1.1	0.3	0.3
11	1,9-	-7.8	14.7	14.7	116.8	180.0	14.4	14.4	25.8	25.8	27.2	27.2
12	2,3-	-17.4	5.2	5.4	108.5	169.4	5.4	6.2	10.9	6.9	13.0	7.4
13	2,4-	-18.8	3.7	5.0	107.6	168.1	4.4	5.6	7.5	8.4	9.1	9.0
14	2,6-	-20.4	2.2	2.2	104.8	165.1	3.0	3.0	5.5	5.5	7.0	7.0
15	2,7-	-25.3	-2.7	-2.7	99.9	160.3	-1.8	-1.8	-1.4	-1.4	-0.1	-0.1
16	2,8-	-24.8	-2.2	-2.2	102.1	164.2	-0.9	-0.9	-0.2	-0.2	0.7	0.7
17	3,4-	-14.7	7.9	8.1	112.1	173.9	7.4	8.2	15.1	11.1	17.6	12.0
18	3,6-	-20.6	2.0	2.0	104.6	164.9	2.4	2.4	4.8	4.8	6.6	6.6
19	3,7-	-25.5	-2.9	-2.9	101.4	163.5	-2.4	-2.4	-2.0	-2.0	-0.6	-0.6
20	4,6-	-15.3	7.2	7.2	111.6	173.7	7.6	7.6	12.3	12.3	14.2	14.2
21	1,2,3-	-44.1	-17.8	-19.8	88.8	153.8	-19.8	-20.3	-2.0	-13.5	2.4	-12.4
22	1,2,4-	-45.9	-19.7	-19.6	88.5	153.0	-21.0	-20.3	-6.4	-10.8	-2.5	-10.0
23	1,2,6-	-48.6	-22.3	-22.1	86.0	150.7	-23.4	-22.6	-9.7	-13.7	-6.1	-11.7
24	1,2,7-	-53.9	-27.7	-27.5	80.6	145.2	-28.7	-27.9	-17.2	-21.2	-13.7	-19.3
25	1,2,8-	-53.1	-26.8	-26.6	81.5	146.1	-27.4	-26.6	-15.5	-19.5	-12.3	-17.9
26	1,2,9-	-29.1	-2.8	-2.6	104.0	167.1	-3.8	-3.0	14.2	10.2	17.4	11.8
27	1,3,4-	-46.0	-19.7	-19.6	88.6	153.2	-21.2	-20.5	-7.9	-12.3	-3.9	-11.4
28	1,3,6-	-53.0	-26.8	-25.5	82.2	146.4	-27.1	-25.9	-19.2	-18.3	-16.0	-16.1
29	1,3,7-	-58.3	-32.0	-30.7	77.0	141.2	-32.4	-31.2	-26.6	-25.7	-23.6	-23.7
30	1,3,8-	-58.2	-31.9	-30.6	77.1	141.2	-32.1	-30.9	-25.4	-24.5	-22.4	-22.5
31	1,3,9-	-37.0	-10.7	-9.4	97.4	160.5	-11.4	-10.2	0.6	1.5	3.7	3.6
32	1,4,6-	-48.6	-22.3	-24.6	83.1	147.3	-22.9	-25.3	-12.3	-14.3	-9.1	-12.1
33	1,4,7-	-54.2	-28.0	-30.3	77.4	141.5	-28.6	-31.0	-20.3	-22.3	-17.3	-20.3
34	1,4,8-	-53.6	-27.4	-29.7	77.9	142.0	-27.6	-30.0	-18.9	-20.9	-16.1	-19.1
35	1,4,9-	-31.7	-5.4	-7.7	99.0	162.1	-6.1	-8.5	8.1	6.1	11.0	8.0
36	1,6,7-	-49.6	-23.3	-23.1	85.2	149.9	-24.5	-23.7	-11.9	-15.9	-8.3	-13.9
37	1,6,8-	-53.0	-26.8	-25.5	82.3	146.5	-26.8	-25.6	-18.8	-17.9	-15.8	-15.9
38	1,7,8-	-52.2	-25.9	-25.7	82.1	146.3	-26.5	-25.7	-16.0	-20.0	-12.5	-18.1
39	2,3,4-	-35.7	-9.5	-11.5	96.3	160.6	-10.7	-11.2	3.4	-8.1	7.6	-7.2
40	2,3,6-	-42.9	-16.6	-16.4	91.7	156.3	-16.5	-15.7	-8.7	-12.7	-5.3	-10.9
41	2,3,7-	-47.8	-21.5	-21.3	86.1	150.0	-21.4	-20.6	-15.8	-19.8	-12.5	-18.1
42	2,3,8-	-47.0	-20.8	-20.7	86.7	150.5	-20.3	-19.5	-14.6	-18.6	-11.7	-17.3
43	2,4,6-	-43.6	-17.3	-16.0	91.4	155.1	-16.8	-15.6	-11.2	-10.3	-8.2	-8.3
44	2,4,7-	-48.8	-22.5	-21.2	86.5	150.6	-22.0	-20.8	-18.9	-18.0	-16.0	-16.1
45	2,4,8-	-48.4	-22.2	-20.9	86.9	151.1	-21.2	-20.0	-17.8	-16.9	-15.3	-15.4
46	2,6,7-	-44.8	-18.5	-18.3	89.4	153.6	-18.8	-18.0	-10.6	-14.6	-7.3	-12.9
47	3,4,6-	-39.8	-13.5	-13.3	94.5	158.6	-14.2	-13.4	-3.9	-7.9	0.0	-5.6
48	3,4,7-	-45.0	-18.7	-18.5	89.6	154.2	-19.3	-18.5	-11.3	-15.3	-7.8	-13.4
49	1,2,3,4-	-60.7	-30.7	-31.4	82.5	151.5	-34.0	-32.1	-7.7	-23.0	-1.2	-21.9
50	1,2,3,6-	-68.5	-38.5	-40.5	72.9	141.5	-40.4	-40.9	-21.0	-32.5	-15.3	-30.1
51	1,2,3,7-	-73.9	-43.9	-45.9	67.5	136.0	-45.7	-46.2	-28.6	-40.1	-23.0	-37.8
52	1,2,3,8-	-73.2	-43.2	-46.2	67.1	135.5	-44.6	-45.1	-27.0	-38.5	-21.6	-36.4
53	1,2,3,9-	-49.8	-19.8	-21.8	90.1	157.1	-22.0	-22.5	2.4	-9.1	7.8	-7.0
54	1,2,4,6-	-69.7	-39.8	-39.7	73.2	141.3	-41.0	-40.3	-24.6	-29.0	-19.2	-26.7
55	1,2,4,7-	-75.4	-45.4	-45.3	67.7	135.7	-46.7	-46.0	-32.8	-37.2	-27.6	-35.1
56	1,2,4,8-	-74.7	-44.7	-44.6	68.2	136.2	-45.5	-44.8	-31.1	-35.5	-26.2	-33.7
57	1,2,4,9-	-51.0	-21.1	-21.0	90.6	157.3	-22.5	-21.8	-1.1	-5.5	3.5	-4.0
58	1,2,6,7-	-72.5	-42.6	-42.2	71.0	139.4	-44.4	-42.8	-25.9	-33.9	-20.4	-31.6
59	1,2,6,8-	-76.0	-46.0	-44.5	68.4	136.5	-46.6	-44.6	-32.6	-35.7	-27.7	-33.4
60	1,2,6,9-	-52.3	-22.3	-24.4	87.1	153.7	-23.5	-25.1	-2.7	-8.7	1.7	-6.9
61	1,2,7,8-	-75.1	-45.1	-44.7	68.6	137.0	-46.3	-44.7	-29.9	-37.9	-24.6	-35.8
62	1,2,7,9-	-57.8	-27.8	-26.3	85.5	152.3	-29.1	-27.1	-10.5	-13.6	-5.7	-11.4
63	1,2,8,9-	-49.4	-19.4	-19.0	93.6	161.3	-20.9	-19.3	3.8	-4.2	8.5	-2.7
64	1,3,4,6-	-70.6	-40.7	-40.6	72.3	140.3	-42.3	-39.9	-26.0	-30.4	-20.6	-28.1
65	1,3,4,7-	-76.2	-46.3	-46.2	66.6	134.5	-47.9	-47.2	-34.0	-38.4	-28.8	-36.3
66	1,3,4,8-	-75.5	-45.6	-45.5	67.4	135.5	-46.8	-46.1	-32.6	-37.0	-27.8	-35.3
67	1,3,4,9-	-55.2	-25.2	-25.1	86.9	154.1	-27.2	-26.5	-6.7	-11.1	-1.7	-9.2
68	1,3,6,7-	-77.3	-47.3	-45.8	67.1	135.1	-48.8	-46.8	-35.2	-38.3	-30.2	-35.9
69	1,3,6,8-	-80.8	-50.8	-48.2	64.4	132.0	-51.1	-48.7	-42.1	-40.3	-37.6	-37.8
70	1,3,6,9-	-60.1	-30.1	-31.1	80.5	147.1	-31.0	-32.2	-16.3	-17.4	-11.7	-14.8
71	1,3,7,8-	-80.0	-50.0	-48.5	64.4	132.4	-50.8	-48.8	-39.5	-42.6	-34.6	-40.3
72	1,3,7,9-	-65.6	-35.6	-33.0	80.4	148.8	-36.6	-34.2	-23.7	-21.9	-19.1	-19.3
73	1,4,6,7-	-72.3	-42.3	-44.4	68.5	136.5	-43.8	-45.4	-28.4	-34.4	-23.2	-31.8
74	1,4,6,8-	-75.8	-45.8	-46.8	65.7	133.3	-46.1	-47.3	-35.2	-36.3	-30.5	-33.6
75	1,4,6,9-	-54.2	-24.2	-28.8	84.5	152.9	-25.1	-29.9	-8.0	-12.0	-3.6	-9.6
76	1,4,7,8-	-75.4	-45.4	-47.5	65.3	133.2	-46.1	-47.7	-33.1	-39.1	-28.1	-36.7
77	1,6,7,8-	-64.4	-34.4	-36.4	76.7	144.9	-36.6	-37.1	-22.8	-34.3	-17.3	-32.1
78	2,3,4,6-	-60.3	-30.4	-32.4	80.7	148.9	-31.8	-32.3	-15.0	-26.5	-9.3	-24.1
79	2,3,4,7-	-65.5	-35.6	-37.6	75.4	143.5	-36.9	-37.4	-22.6	-34.1	-17.2	-32.0
80	2,3,4,8-	-65.3	-35.3	-37.3	76.1	144.6	-36.2	-37.8	-21.7	-33.2	-16.4	-31.2
81	2,3,6,7-	-66.7	-36.8	-36.4	76.6	144.6	-37.8	-36.2	-24.4	-32.4	-19.1	-30.3
82	2,3,6,8-	-70.5	-40.5	-39.0	73.6	141.2	-40.4	-38.4	-31.7	-34.8	-26.9	-32.6

TABLE 4: Continued

no.	PCDFs	G3XMP2				MP2		DFT/L		DFT/S		
		AR	IR1	IR2	G-298	G-600	IR1	IR2	IR1	IR2	IR1	IR2
83	2,3,7,8-	-69.4	-39.4	-39.0	75.7	145.5	-39.7	-38.1	-28.6	-36.6	-23.6	-34.8
84	2,4,6,7-	-67.7	-37.7	-36.2	76.4	144.1	-38.3	-36.2	-27.0	-30.1	-22.0	-27.7
85	2,4,6,8-	-71.3	-41.3	-38.7	75.2	144.1	-40.7	-38.3	-33.9	-32.1	-29.7	-29.9
86	3,4,6,7-	-63.7	-33.7	-33.3	81.4	151.2	-35.5	-33.9	-19.6	-27.6	-13.9	-25.1
87	1,2,3,4,6-	-85.1	-51.4	-52.1	66.4	138.8	-54.9	-53.0	-25.7	-41.0	-17.4	-38.1
88	1,2,3,4,7-	-90.7	-57.0	-57.7	60.9	133.2	-60.5	-58.6	-33.8	-49.1	-25.8	-46.5
89	1,2,3,4,8-	-90.0	-56.3	-57.0	61.7	134.1	-59.4	-57.5	-32.2	-47.5	-24.6	-45.3
90	1,2,3,4,9-	-66.5	-32.8	-33.5	83.6	154.5	-36.6	-34.7	-2.5	-17.8	5.1	-15.6
91	1,2,3,6,7-	-92.8	-59.1	-60.9	57.7	130.0	-62.0	-61.7	-36.8	-52.3	-29.1	-49.5
92	1,2,3,6,8-	-96.2	-62.5	-63.2	55.0	126.9	-64.2	-63.5	-43.5	-54.1	-36.3	-51.2
93	1,2,3,6,9-	-72.5	-38.9	-43.2	73.4	143.8	-41.2	-44.1	-14.0	-27.5	-7.1	-24.9
94	1,2,3,7,8-	-95.5	-61.8	-63.6	55.0	127.3	-64.0	-63.7	-41.0	-56.5	-33.4	-53.8
95	1,2,3,7,9-	-78.1	-44.4	-45.1	71.7	142.2	-46.8	-46.1	-21.7	-32.3	-14.5	-29.4
96	1,2,3,8,9-	-69.8	-36.1	-37.9	77.9	147.5	-38.8	-38.5	-7.6	-23.1	-0.5	-20.9
97	1,2,4,6,7-	-93.9	-60.2	-59.9	58.2	130.2	-62.6	-61.1	-40.5	-48.9	-33.0	-46.1
98	1,2,4,6,8-	-97.0	-63.3	-61.9	55.8	127.3	-64.4	-62.5	-46.8	-50.3	-40.0	-47.6
99	1,2,4,6,9-	-73.5	-39.8	-42.0	74.0	143.9	-41.5	-43.2	-16.8	-23.2	-10.2	-20.7
100	1,2,4,7,8-	-96.8	-63.2	-62.9	55.2	127.1	-64.8	-63.3	-45.1	-53.5	-37.9	-51.0
101	1,2,4,7,9-	-79.2	-45.5	-44.1	72.4	142.6	-47.2	-45.3	-25.1	-28.6	-18.5	-26.1
102	1,2,4,8,9-	-71.1	-37.4	-37.1	78.7	148.1	-39.4	-37.9	-11.0	-19.4	-4.5	-17.6
103	1,2,6,7,8-	-93.0	-59.3	-61.1	56.9	128.6	-61.8	-61.5	-36.5	-52.0	-28.9	-49.3
104	1,2,6,7,9-	-75.6	-41.9	-41.6	76.0	147.4	-44.4	-42.9	-17.3	-25.7	-10.5	-23.6
105	1,3,4,6,7-	-94.6	-60.9	-60.6	56.2	126.7	-63.6	-62.1	-41.7	-50.1	-34.2	-47.3
106	1,3,4,6,8-	-98.1	-64.4	-63.0	55.1	127.0	-65.9	-64.0	-48.6	-52.1	-41.5	-49.1
107	1,3,4,6,9-	-77.2	-43.5	-45.7	71.1	141.6	-45.6	-47.3	-22.4	-28.8	-15.5	-26.0
108	1,3,4,7,8-	-97.5	-63.8	-63.5	53.3	124.0	-65.8	-64.3	-46.4	-54.8	-39.4	-52.5
109	1,3,4,7,9-	-83.0	-49.3	-47.9	70.3	142.3	-51.5	-49.6	-30.6	-34.1	-23.7	-31.3
110	1,3,6,7,8-	-97.7	-64.0	-64.7	53.2	124.8	-66.2	-65.5	-45.9	-56.5	-38.6	-53.5
111	1,4,6,7,8-	-92.7	-59.0	-63.3	54.8	126.8	-61.2	-64.1	-39.0	-52.5	-31.5	-49.3
112	2,3,4,6,7-	-84.2	-50.5	-52.3	65.9	137.9	-53.0	-52.7	-30.6	-46.1	-22.6	-43.0
113	2,3,4,6,8-	-87.8	-54.1	-54.8	63.3	135.1	-55.4	-54.7	-37.6	-48.2	-30.4	-45.3
114	2,3,4,7,8-	-87.1	-53.4	-55.2	63.3	135.7	-55.2	-54.9	-35.0	-50.5	-27.7	-48.1
115	1,2,3,4,6,7-	-109.1	-71.7	-72.2	51.6	127.8	-76.3	-73.6	-41.4	-60.7	-31.0	-57.3
116	1,2,3,4,6,8-	-112.2	-74.8	-74.2	49.2	125.1	-78.1	-75.0	-47.8	-62.2	-38.0	-58.8
117	1,2,3,4,6,9-	-88.6	-51.2	-54.2	67.6	141.9	-55.2	-55.7	-17.8	-35.1	-8.2	-31.9
118	1,2,3,4,7,8-	-112.0	-74.6	-75.1	48.7	125.0	-78.5	-75.8	-45.9	-65.2	-35.9	-62.2
119	1,2,3,4,7,9-	-94.3	-56.9	-56.3	65.7	140.1	-61.0	-57.9	-26.1	-40.5	-16.6	-37.4
120	1,2,3,4,8,9-	-86.2	-48.8	-49.3	71.4	144.5	-53.1	-50.4	-12.1	-31.4	-2.7	-29.0
121	1,2,3,6,7,8-	-113.0	-75.6	-79.6	44.2	120.4	-79.3	-77.7	-47.2	-60.2	-37.1	-66.7
122	1,2,3,6,7,9-	-95.5	-58.1	-60.0	61.9	136.2	-61.8	-59.8	-28.3	-44.2	-18.9	-41.2
123	1,2,3,6,8,9-	-91.1	-53.7	-55.6	64.8	137.6	-56.9	-54.9	-21.9	-37.8	-12.9	-35.2
124	1,2,3,7,8,9-	-90.1	-52.7	-56.7	65.7	140.6	-56.6	-55.0	-18.6	-41.6	-9.1	-37.7
125	1,2,4,6,7,8-	-113.8	-76.4	-78.3	45.1	121.0	-79.4	-77.4	-50.5	-66.4	-40.8	-63.1
126	1,2,4,6,7,9-	-96.2	-58.9	-58.7	62.8	136.8	-61.8	-59.4	-30.9	-39.7	-22.0	-37.0
127	1,2,4,6,8,9-	-91.8	-54.4	-54.2	67.5	141.7	-56.8	-54.4	-24.5	-33.3	-16.0	-31.0
128	1,3,4,6,7,8-	-114.5	-77.1	-79.0	44.3	120.2	-80.5	-78.5	-52.1	-68.0	-42.3	-64.6
129	1,3,4,6,7,9-	-99.8	-62.4	-62.2	61.6	137.9	-65.8	-63.4	-36.4	-45.2	-27.2	-42.2
130	2,3,4,6,7,8-	-104.1	-66.7	-70.7	54.5	132.1	-69.9	-68.3	-40.9	-63.9	-30.9	-60.5
131	1,2,3,4,6,7,8-	-128.8	-87.7	-90.4	38.7	118.9	-93.0	-91.6	-51.3	-78.1	-38.6	-74.1
132	1,2,3,4,6,7,9-	-111.1	-70.0	-70.6	56.5	134.7	-75.3	-72.7	-31.7	-51.4	-19.8	-48.0
133	1,2,3,4,6,8,9-	-106.7	-65.6	-66.2	58.7	134.6	-70.4	-68.8	-25.3	-44.9	-13.7	-41.9
134	1,2,3,4,7,8,9-	-106.0	-64.9	-67.6	58.0	134.7	-70.3	-68.9	-22.7	-49.6	-10.7	-46.2
135	octa-	-121.7	-76.9	-78.3	52.8	133.7	-84.0	-80.2	-25.7	-56.3	-11.3	-52.7

^a MP2 = MP2/G3MP2Large, DFT/L = B3LYP/6-311++G(3df,3pd), DFT/S = B3LYP/6-31G(2df,p), AR = atomization reaction, IR1/IR2 = isodesmic reaction IR1/IR2, G-298 and G-600: the standard Gibbs free energy at 298 and 600 K, all based on the enthalpies of formation from G3XMP2//IR2 and thermodynamic parameters from CODATA for elements.

values are ca. 20 kJ/mol higher than those from G3X and G3XMP2. Because the theoretical studies cannot reach a consistent value for $\Delta_f H_{298K}^o$ (DBF) and the better determination of sublimation enthalpy by Verevkin, we will use the value of 52.90 ± 0.65 kJ/mol by Verevkin⁴¹ in the isodesmic calculations, while previous theoretical predictions of formation enthalpies of PCDFs^{11,19,27} have used the value by Chirico et al.

C. Enthalpies of Formation of PCDFs. $\Delta_f H_{298K}^o$ (PCDFs) can be obtained directly from G3XMP2 atomization energies, however, with fairly large deviations as evidenced in the cases of PCDDs³¹ and DBF. $\Delta_f H_{298K}^o$ (DBF) = 37.7 kJ/mol from G3XMP2 atomization energy is significantly different from the experimental value of 52.90 ± 0.65 kJ/mol. It is therefore necessary to employ isodesmic reactions. Here we have employed isodesmic reactions IR1 and IR2 at levels of G3XMP2, MP2/G3MP2Large, B3LYP/6-311++G(3df,3pd), and B3LYP/6-31G(2df,p), all based on the B3LYP/6-31G(2df,p) geometries and ZPE corrections. The values of $\Delta_f H_{298K}^o$ are listed

in Table 3 and the G3XMP2//IR2 values are plotted in Figure 2a. Also plotted in Figure 2a are the differences of B3LYP, MP2, and PM3 predictions to G3XMP2 ones. The values obtained from G3XMP2 calculations with reactions IR1 and IR2 agree closely within 4 kJ/mol for all PCDFs except for 1,4,6,9-T₄CDF, 1,2,3,6,9-P₅CDFs, and 1,4,6,7,8-P₅CDFs.

Compared to G3XMP2, DFT-B3LYP significantly overpredicts the enthalpies of formation and the differences increase with the degree of chlorination. Our DFT-B3LYP calculations agree closely with the previous B3LYP studies with different basis sets. For example, $\Delta_f H_{298K}^o$ (4,6-D₂CDF) was obtained at the B3LYP level as 9.8 kJ/mol with 6-31G(d),²⁹ 12.7 kJ/mol with 6-311+G(3df,2p),²⁶ 14.2 kJ/mol with 6-31G(2df,p), and 12.3 kJ/mol with 6-311++G(3df,3pd) in the present study, all using isodesmic reaction IR1. For $\Delta_f H_{298K}^o$ (O₈CDF), the value changes from -14.9 kJ/mol with the 6-31G(d) basis set²⁹ to the present -25.7 kJ/mol with 6-311++G(3df,3pd). With reaction IR1, increasing the basis set from 6-31G(2df,p) to

TABLE 5: The Positional Interactions for PCDDs (all in kJ/mol)^a

	G3XMP2 //IR1	DFT/S // IR1	DFT/L //IR1	MP2//IR1
χ_0	47.51	45.49	46.44	48.75
χ_1	-29.40	-24.57	-25.91	-30.21
χ_2	-27.00	-25.36	-26.28	-26.76
χ_3	-23.78	-20.25	-21.60	-24.32
χ_4	-20.70	-16.12	-17.51	-21.32
ClCl ₁₂	6.77	13.28	12.54	6.06
ClCl ₁₃	0.89	1.72	1.47	0.53
ClCl ₁₄	1.50	2.35	2.23	1.40
ClCl ₁₆	0.42	0.87	0.80	0.57
ClCl ₁₇	-0.76	-0.60	-0.74	-0.48
ClCl ₁₈	1.18	1.07	1.12	1.04
ClCl ₁₉	25.91	28.32	28.74	26.13
ClCl ₂₃	3.78	6.21	5.83	3.25
ClCl ₂₄	2.47	3.24	2.95	2.16
ClCl ₂₆	0.27	0.70	0.60	0.37
ClCl ₂₇	0.35	1.11	0.95	0.59
ClCl ₂₈	1.02	0.17	0.24	1.02
ClCl ₃₄	3.78	6.21	5.83	3.26
ClCl ₃₆	1.31	2.38	2.13	1.25
ClCl ₃₇	0.41	0.16	0.14	0.32
ClCl ₄₆	1.56	2.95	2.66	1.77

^a DFT/S = B3LYP/6-31G(2df,p), DFT/L = B3LYP/6-311++G(3df,3pd), MP2 = MP2/G3MP2Large; χ_n are the primary substitution effects ($n = 1-4$), ClCl_{mn} are the secondary interactions between chlorination substitutions at sites m and n ($m, n = 1-4$ and 5-9).

6-311++G(3df,3pd) improves the performance of DFT-B3LYP only slightly. On the other hand, employing isodesmic reaction IR2 can greatly improve the agreement of B3LYP to G3XMP2, e.g., $\Delta_f H_{298K}^{\circ}(O_8CDF) = -56.3$ kJ/mol from B3LYP/6-311++G(3df,3pd)//IR2 is comparable to -78.3 kJ/mol from G3XMP2//IR2. Shibata et al.³⁰ have used a similar approach by setting corrections to a different number of chlorinations, and obtained $\Delta_f H_{298K}^{\circ}(\text{octa-CDF}) = -60$ kJ/mol at the B3LYP/6-31G(d) level, agreeing with our isodesmic IR2 result.

On the other hand, MP2/G3MP2Large agrees closely with G3XMP2, using both IR1 and IR2. The agreements between MP2 and G3XMP2 are within 2.5 kJ/mol with IR2 and within 5 kJ/mol with IR1 from M₁CDFs to H₆CDFs. With IR1, the difference between MP2 and G3XMP2 increases to 7.1 kJ/mol for O₈CDF. Similar performance of MP2/G3MP2Large was also observed in predictions on PCDDs, where the largest difference was 5.4 kJ/mol for O₈CDD with similar isodesmic reaction to IR1.

The relative stabilities of isomers are described by using the positional interactions: the primary substitutions of Cl at four different sites (χ_1 , χ_2 , χ_3 , and χ_4) and the secondary two-body Cl–Cl interactions. The parameters obtained from linear regression are given in Table 3. While substitution at position 1/9 leads to more stable congeners than those at other positions, the simultaneous Cl-substitution at positions 1 and 9 introduces a much large instability because of the strong repulsive interactions between Cl-atoms. The Cl₁–Cl₉ distances are rather short, e.g., 3.249 Å in 1,9-Di-CDF and 3.173 Å in octa-CDF at the B3LYP/6-31G(2df,p) level, compared to the other three vicinal Cl–Cl distances of 3.188 Å of Cl₁–Cl₂, 3.117 Å of Cl₂–Cl₃, and 3.065 Å of Cl₃–Cl₄ in octa-CDF. The other significant repulsive interactions are those between vicinal Cl-atoms, most notably at positions 1 and 2 (or 8 and 9). Other inter-ring interactions are less important. The regression on B3LYP/6-311++G(3df,3pd)//IR1 results also shows that the overpredictions are primarily due to the underestimation of substitutions on position 1 and 4 and the overestimation of Cl–Cl repulsion, especially to the *o*-ClCl interactions.

D. Isomer Patterns and Thermodynamics. To assess the role of thermodynamic properties in PCDD/F formation processes, the standard Gibbs free energies at 298 and 600 K are calculated (Table 4) and plotted in Figure 2b. The most abundant congeners at 600 K, according to the Gibbs free energies, are 1-, 1,7-/1,8-, 1,3,7-/1,3,8-/1,4,7-/1,4,8-, 1,3,6,8-/1,3,7,8-/1,4,7,8-/1,4,6,8-, 1,3,4,7,8-/1,3,6,7,8-, 1,3,4,6,7,8-/1,2,3,6,7,8-/1,2,4,6,7,8-, and 1,2,3,4,6,7,8-PCDFs. Thermodynamic isomer patterns at 600 K are predicted here for T₄CDF, H₆CDF, and H₇CDF.

Formations of PCDD/Fs in de novo synthesis from chlorination of PAH³ and in condensation of chlorinated phenols⁴ show specific isomer patterns which cannot be accounted for thermodynamically because of the distinctive formation mechanism. For example, Weber et al.³ observed larger abundance of 1,2,3,4,6,7,9-H₇CDF than that of 1,2,3,4,6,7,8-H₇CDF from a de novo experiment of a PAH mixture, while the pure thermodynamic percentages of 1,2,3,4,6,7,9- and 1,2,3,4,6,7,8-H₇CDF are ca. 4% and 88%, respectively, at 600 K; and the predominant 2,4,6-, 2,4,7-, 3,4,6-, and 3,4,7-T₃CDFs are no more thermodynamically favored than the stable congeners of 1,3,7-, 1,3,8-, 1,4,7-, and 1,4,8-T₃CDFs.

On the other hand, the PCDF isomer patterns from MWI flue-gas samples can be approximately accounted for by chlorination of DBF and/or dechlorination of O₈CDF on fly ashes,⁵⁻⁷ where the gas-phase phenol condensation acts as a source of DBF,⁷ and chlorination of graphite as a source of O₈CDF.⁵ For the chlorination process, Ryu et al.⁴³ have assigned chlorination probabilities of 0.154, 0.273, 0.350, and 0.223 at sites 1/9, 2/8, 3/7, and 4/6, which are different from the thermodynamic ones of 0.464, 0.221, 0.230, and 0.084. On the other hand, the dechlorination processes follow roughly the thermodynamic propensity. Figure 3a shows that H₇CDFs appear to have thermodynamically controlled isomer distributions in incineration ashes and fly ashes,^{8,44} and H₆CDFs in the flue gas.^{7,45} However, H₆CDF isomer distributions from fly ashes show large deviation to thermodynamic distribution (Figure 3b),^{8,44} where $\Delta_f G_{600K}^{\circ}$ overpredicts the percentage for 1,2,3,6,7,8-H₆CDF and underestimates that for 2,3,4,6,7,8-H₆CDF. For T₄CDF (Figure 3c), there are even larger discrepancies between theory and experiments, e.g., on 1,2,3,4- + 2,3,4,9-T₄CDF and 3,4,6,7-T₄CDF. Addink et al.⁸ have obtained similar results using empirical thermodynamic parameters. The comparisons suggest that the thermodynamic control may play an important role in the formation of PCDFs by dechlorination, while they also suggest effects from the kinetics of chlorination and dechlorination processes.

Acknowledgment. We thank the computing platform SCUT-Grid from Information Network Research and Engineering Centre of South China University of Technology for service support and the NSFC (No. 20777017) for financial support.

Supporting Information Available: The rotational constants and vibrational frequencies of the PCDDs at the B3LYP/6-31G(2df,p) level are available in Microsoft Excel format. This material is available free of charge via the Internet at <http://pubs.acs.org>.

References and Notes

- Shaub, W. M.; Tsang, W. *Environ. Sci. Technol.* **1983**, *17*, 721. Froese, K. L.; Hutzinger, O. *Environ. Sci. Technol.* **1996**, *30*, 1009. Froese, K. L.; Hutzinger, O. *Environ. Sci. Technol.* **1996**, *30*, 998. Ryu, J.-Y.; Choi, K.-C.; Mulholland, J. A. *Chemosphere* **2006**, *65*, 1526. Wiater-Protas, I.; Louw, R. *Eur. J. Org. Chem.* **2001**, 3945. Tuppurainen, K.; Asikainen, A.; Ruokoljarvi, P.; Ruuskanen, J. *Acc. Chem. Res.* **2003**, *36*, 652. de Jong, V.; Cieplik, M. K.; Louw, R. *Environ. Sci. Technol.* **2004**, *38*, 5217.

- (2) Xhouret, C.; Pirard, C.; de Pauw, E. *Environ. Sci. Technol.* **2001**, *35*, 1616.
- (3) Weber, R.; Iino, F.; Imagawa, T.; Takeuchi, M.; Sakurai, T.; Sadakata, M. *Chemosphere* **2001**, *44*, 1429.
- (4) Ryu, J.-Y.; Mulholland, J. A.; Oh, J.-E.; Nakahata, D. T.; Kim, D. H. *Chemosphere* **2004**, *55*, 1447. Ryu, J.-Y.; Mulholland, J. A.; Takeuchi, M.; Kim, D. H.; Hatanaka, T. *Chemosphere* **2005**, *61*, 1312.
- (5) Iino, F.; Tsuchiya, K.; Imagawa, T.; Gullett, B. K. *Environ. Sci. Technol.* **2000**, *34*, 3143.
- (6) Weber, R.; Nagai, K.; Nishino, J.; Shiraishi, H.; Ishida, M.; Takasuga, T.; Konndo, K.; Hiraoka, M. *Chemosphere* **2002**, *46*, 1247. Weber, R.; Takasuga, T.; Nagai, K.; Shiraishi, H.; Sakurai, T.; Matuda, T.; Hiraoka, M. *Chemosphere* **2002**, *46*, 1225.
- (7) Ryu, J.-Y.; Mulholland, J. A.; Dunn, J. E.; Iino, F.; Gullett, B. K. *Environ. Sci. Technol.* **2005**, *39*, 4398.
- (8) Addink, R.; Govers, H. A. J.; Olie, K. *Environ. Sci. Technol.* **1998**, *32*, 1888.
- (9) Tan, P.; Hurtado, I.; Neuschutz, D.; Eriksson, G. *Environ. Sci. Technol.* **2001**, *35*, 1867.
- (10) Okamoto, Y.; Tomonari, M. *J. Phys. Chem. A* **1999**, *103*, 7686. Murabayashi, M.; Moesta, H. *Environ. Sci. Technol.* **1992**, *26*, 797.
- (11) Burcat, A.; Khachatryan, L.; Dellinger, B. L. *J. Phys. Chem. Ref. Data* **2003**, *32*, 443.
- (12) Khachatryan, L.; Asatryan, R.; Dellinger, B. L. *Chemosphere* **2003**, *52*, 695. Khachatryan, L.; Burcat, A.; Dellinger, B. L. *Combust. Flame* **2003**, *132*, 406.
- (13) Lukyanova, V. A.; Kolesov, V. P.; Avramenko, N. V.; Vorobiera, V. P.; Golovkov, V. F. *Russ. J. Phys. Chem. (Engl. Transl.)* **1997**, *71*, 338. Papina, T. S.; Kolesov, V. P.; Lukyanova, V. A.; Golovkov, V. F.; Chernov, C. A.; Vorobiera, V. P. *J. Chem. Thermodyn.* **1998**, *30*, 431. Papina, T. S.; Kolesov, V. P.; Vorobiera, V. P.; Folovkov, V. F. *J. Chem. Thermodyn.* **1996**, *28*, 307. Papina, T. S.; Lukyanova, V. A.; Kolesov, V. P.; Golovkov, V. F.; Chernov, C. A.; Vorobiera, V. P. *Zh. Fiz. Khim.* **1998**, *72*, 1.
- (14) Klots, T. D.; Collier, W. B. *J. Mol. Struct.* **1996**, *380*, 1.
- (15) Cass, R. C.; Fletcher, S. E.; Mortimer, C. T.; Soringall, H. D.; White, T. R. *J. Chem. Soc.* **1958**, 1406.
- (16) Sabbah, R.; Antipine, I. *Bull. Soc. Chim. Fr.* **1987**, 392. Sabbah, R. *Bull. Soc. Chim. Fr.* **1991**, 350.
- (17) Chirico, R. D.; Gammon, B. E.; Knipmeyer, S. E.; Nguyen, A.; Strube, M. M.; Tsionopoulos, C.; Steele, W. V. *J. Chem. Thermodyn.* **1990**, *22*, 1075.
- (18) Shaub, W. M. *Thermochim. Acta* **1983**, *62*, 315.
- (19) Thompson, D. *Chemosphere* **1994**, *29*, 2583.
- (20) Thompson, D. *Thermochim. Acta* **1995**, *261*, 7.
- (21) Dorofeeva, O. V.; Gurvich, V. L. *Zh. Fiz. Khim.* **1996**, *70*, 7.
- (22) Thompson, D.; Ewan, B. C. *J. Phys. Chem. A* **2007**, *111*, 5043.
- (23) Koester, C. J.; Hites, R. A. *Chemosphere* **1988**, *17*, 2355.
- (24) Unsworth, J.-F.; Dorans, H. *Chemosphere* **1993**, *27*, 351.
- (25) Saito, N.; Fuwa, A. *Chemosphere* **2000**, *40*, 131.
- (26) Zhu, L.; Bozzelli, J. W. *J. Phys. Chem. Ref. Data* **2003**, *32*, 1713.
- (27) Dorofeeva, O. V.; Iorish, V. S.; Moiseeva, N. F. *J. Chem. Eng. Data* **1999**, *44*, 516.
- (28) Leon, L. A.; Notario, R.; Quijano, J.; Sanchez, C. *J. Phys. Chem. A* **2002**, *106*, 6618. Lee, J. E.; Choi, W.; Mhin, B. J. *J. Phys. Chem. A* **2003**, *107*, 2693. Wang, Z.-Y.; Zhai, Z.-C.; Wang, L.-S.; Chen, J.-L.; Kikuchi, O.; Watanabe, T. *J. Mol. Struct. (THEOCHEM)* **2004**, *672*, 97. Dorofeeva, O. V.; Yungman, V. S. *J. Phys. Chem. A* **2003**, *107*, 2848.
- (29) Wang, Z.-Y.; Zhai, Z.-C.; Wang, L.-S. *J. Mol. Struct. (THEOCHEM)* **2005**, *725*, 55.
- (30) Shibata, E.; Yamamoto, S.; Koyo, H.; Ikeda, T.; Kasai, E.; Maeda, M.; Nakamura, T. *Mater. Trans.* **2001**, *42*, 2531.
- (31) Wang, L.; Pilling, M. J.; Heard, D. E.; Seakins, P. *J. Phys. Chem. A* **2008**, *112*, 1832.
- (32) Curtiss, L. A.; Redfern, P. C.; Raghavachari, K.; Pople, J. A. *J. Chem. Phys.* **2001**, *114*, 108.
- (33) Frisch, M. J.; Trucks, G. W.; Schlegel, H. B.; Scuseria, G. E.; Robb, M. A.; Cheeseman, J. R.; Montgomery, J. A., Jr.; Vreven, T.; Kudin, K. N.; Burant, J. C.; Millam, J. M.; Iyengar, S. S.; Tomasi, J.; Barone, V.; Mennucci, B.; Cossi, M.; Scalmani, G.; Rega, N.; Petersson, G. A.; Nakatsuji, H.; Hada, M.; Ehara, M.; Toyota, K.; Fukuda, R.; Hasegawa, J.; Ishida, M.; Nakajima, T.; Honda, Y.; Kitao, O.; Nakai, H.; Klene, M.; Li, X.; Knox, J. E.; Hratchian, H. P.; Cross, J. B.; Bakken, V.; Adamo, C.; Jaramillo, J.; Gomperts, R.; Stratmann, R. E.; Yazyev, O.; Austin, A. J.; Cammi, R.; Pomelli, C.; Ochterski, J. W.; Ayala, P. Y.; Morokuma, K.; Voth, G. A.; Salvador, P.; Dannenberg, J. J.; Zakrzewski, V. G.; Dapprich, S.; Daniels, A. D.; Strain, M. C.; Farkas, O.; Malick, D. K.; Rabuck, A. D.; Raghavachari, K.; Foresman, J. B.; Ortiz, J. V.; Cui, Q.; Baboul, A. G.; Clifford, S.; Cioslowski, J.; Stefanov, B. B.; Liu, G.; Liashenko, A.; Piskorz, P.; Komaromi, I.; Martin, R. L.; Fox, D. J.; Keith, T.; Al-Laham, M. A.; Peng, C. Y.; Nanayakkara, A.; Challacombe, M.; Gill, P. M. W.; Johnson, B.; Chen, W.; Wong, M. W.; Gonzalez, C.; Pople, J. A. *Gaussian 03*, Revision B.05; Gaussian Inc.: Wallingford, CT, 2004.
- (34) Bylaska, E. J.; de Jong, W. A.; Kowalski, K.; Straatsma, T. P.; Valiev, M.; Wang, D.; Apra, E.; Windus, T. L.; Hirata, S.; Hackler, M. T.; Zhao, Y.; Fan, P.-D.; Harrison, R. J.; Dupuis, M.; Smith, D. M. A.; Nieplocha, J.; Tipparaju, V.; Krishnan, M.; Auer, A. A.; Nooijen, M.; Brown, E.; Cisneros, G.; Fann, G. I.; Fruchtl, H.; Garza, J.; Hirao, K.; Kendall, R.; Nichols, J. A.; Tsemekhman, K.; Wolinski, K.; Anchell, J.; Bernholdt, D.; Borowski, P.; Clark, T.; Clerc, D.; Dachs, H.; Deegan, M.; Dyall, K.; Elwood, D.; Glendening, E.; Gutowski, M.; Hess, A.; Jaffe, J.; Johnson, B.; Ju, J.; Kobayashi, R.; Kutteh, R.; Lin, Z.; Littlefield, R.; Long, X.; Meng, B.; Nakajima, T.; Niu, S.; Pollack, L.; Rosing, M.; Sandrone, G.; Stave, M.; Taylor, H.; Thomas, G.; van Lenthe, J.; Wong, A.; Zhang, Z. *NWChem*, A Computational Chemistry Package for Parallel Computers, Version 5.0; Pacific Northwest National Laboratory: Richland, WA, 2006.
- (35) Balint-Kurt, G. G.; Martson, C. C. *J. Chem. Phys.* **1989**, *91*, 3571. Johnson, R. D. I. FGHIID Program (<http://www.nist.gov/compchem/johnson/fgh/fgh1d.html>), 1999.
- (36) Rordorf, B. F. *Chemosphere* **1989**, *18*, 783. Ritter, E. R.; Bozzelli, J. W. *Combust. Sci. Technol.* **1994**, *101*, 153.
- (37) Pedley, J. B. *Thermochemical Data and Structures of Organic and Organometallic Compounds*; Thermodynamics Research Center: College Station, TX, 1994; Vol. 1.
- (38) Cox, J. D.; Pilcher, G. *Thermochemistry of Organic and Organometallic Compounds*; Academic Press: New York, 1970.
- (39) Allinger, N. L.; Yan, L. *J. Am. Chem. Soc.* **1993**, *115*, 11918.
- (40) Notario, R.; Roux, M. V.; Castano, O. *Phys. Chem. Chem. Phys.* **2001**, *3*, 3717.
- (41) Verevkin, S. P. *Phys. Chem. Chem. Phys.* **2003**, *5*, 710.
- (42) Altarawneh, M.; Dlugogorski, B. Z.; Kennedy, E. M.; Mackie, J. C. *J. Phys. Chem. A* **2006**, *110*, 13560.
- (43) Ryu, J.-Y.; Mulholland, J. A.; Dunn, J. E.; Iino, F.; Gullett, B. K. *Environ. Sci. Technol.* **2004**, *38*, 5112.
- (44) Yasuhara, A.; Ito, H.; Morita, M. *Environ. Sci. Technol.* **1987**, *21*, 971.
- (45) Cunliffe, A. M.; Williams, P. T. *Chemosphere* **2007**, *66*, 1929.